Magnetic Zintl Phases

DOI: 10.1002/anie.201209036

Field-Induced Inversion of the Magnetoresistive Effect in the Zintl Phase $Eu_{5+x}Mg_{18-x}Si_{13}$ ($x = 2.2$)**

*Adam Slabon, Christian Mensing, Christof Kubata, Eduardo Cuervo-Reyes, and Reinhard Nesper**

The discovery of giant magnetoresistance (GMR effect)[1] in magnetic multilayers has led to a rapid technological advance in spintronic research and device building, for example, magnetoresistive random-access memory (MRAM). The operating principle is based on the dependence of the electrical resistivity on the spin alignment in the magnetic domains of the material.[2] All ferromagnetic metals exhibit a finite but small change of the electronic conductivity after application of an external magnetic field. The value of the magnetoresistivity *MR* under applied magnetic field *H* is defined as $MR = [\rho(H) - \rho(0)]/\rho(0)] \times 100\,\%$ (ρ = electrical resistivity) and can be either positive or negative. If the resistance drop is associated with critical ferromagnetic fluctuations, this phenomenon is called colossal magnetoresistance (CMR). This effect was observed for the first time for the manganese perovskites $RE_{1-x}B_xMnO_3$ (RE = rare-earth metal; B = divalent cation).[3]

The discovery of enhanced MR, often described as CMR in the literature, for the ternary Zintl phase[4] $Eu_{14}MnSb_{11}$ has led to intensive investigations of this class of compounds.[5] The MR effect occurs simultaneously with ferromagnetic ordering due to the parallel alignment of the unpaired 4f electrons of the rare-earth metals. In the case of Eu^{2+} ions they should contribute with a local magnetic moment of 7.94 μ_B.

We report herein on the synthesis of the new ternary Zintl phase $Eu_{5+x}Mg_{18-x}Si_{13}$ ($x = 2.2$)[6] which displays an unusual MR effect. The title compound does not show a maximum of the resistivity at low temperatures and no saturation at fields up to 6 T. Furthermore, an inversion of the sign of the MR as a function of applied field and temperature can be observed.

The crystal structure of $Eu_{5+x}Mg_{18-x}Si_{13}$ ($x = 2.2$) is depicted in Figure 1. Tetrel compounds such as $M_{5+x}Mg_{18-x}T_{13}$ (M = Sr, Ba; Tt = Si, Ge), which crystallize in their own structure type, have been known for some time.[7] The structure usually contains isolated Si^{4-} anions as well as planar Si_4 clusters for which different valence electron numbers have been found.[7,8] Moreover, the tetrel center of the Tt_4 cluster can be replaced by a metal such as Li or Mg without causing a structural change in the geometrical pattern. Recently, we reported on the synthesis of the phase $Eu_{5+x}Mg_{18-x}Ge_{13}$ ($x = 0.1$), which is isostructural with $Sr_{6.3}Mg_{16.7}Si_{13}$ and isopunctual with $Eu_8Mg_{16}Ge_{12}$. In the new compound the Tt_4 unit collapses into three isolated Tt^{4-} anions by means of such substitution.[9] This indicates the remarkable flexibility of that structure type, which we have tested now by systematic changes of the composition and investigated the related electronic effects.

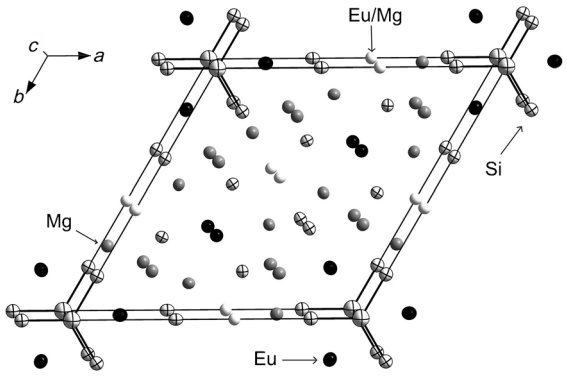

Figure 1. Crystal structure of $Eu_{5+x}Mg_{18-x}Si_{13}$ ($x = 2.2$). The 3f site displaying mixed europium/magnesium occupancy is marked by white balls.

The electronic structure of the title compound can be interpreted according to the Zintl–Klemm concept as $(Eu^{2+})_{5+x}(Mg^{2+})_{18-x}(Si^{4-})_9(Si_4^{10-})$ with nine isolated silicon anions and a planar $[Si_4]$ unit.[6,9] The anisotropic displacement ellipsoid of the central silicon atom exhibits significant elongation in the [001] direction, that is, perpendicular to the anion mean plane and pointing towards a deviation from planarity. However, owing to the small displacement of the $[Si_4]^{10-}$ anion from the plane, the geometry resembles the carbonate anion rather than the isoelectronic pyramidal PCl_3. The bond lengths of 2.56 Å between the terminal and central atom are within the range of elongated single bonds. Similar to many tetrel Zintl phases the anions are ecliptically stacked[7] so that their partially depopulated π^* orbitals interact in the [001] direction over a distance of approximately 4.4 Å. The trigonal-prismatic coordination of the central silicon atom by europium neighbors follows the well-known pattern of Zintl phases containing divalent rare-earth and alkaline-earth metals.[10] The terminal atoms of the Si_4 unit are coordinated by magnesium atoms with contact distances of 2.67 Å. The mixed occupancy of the 3f site by

[*] A. Slabon, Dipl.-Ing. C. Mensing, Dr. C. Kubata, Dr. E. Cuervo-Reyes, Prof. Dr. R. Nesper
Department of Chemistry, ETH Zürich
Wolfgang-Pauli-Strasse 10, CH-8093 Zürich (Switzerland)
E-mail: nesper@inorg.chem.ethz.ch

[**] This work was supported financially by the Swiss National Science Foundation (project no. 2-77937-10) and the ETH Zürich. We thank Dr. Frank Krumeich, Hao Wang, and Dr. Bodo Hattendorf for the chemical analyses.

Supporting information for this article is available on the WWW under http://dx.doi.org/10.1002/anie.201209036.

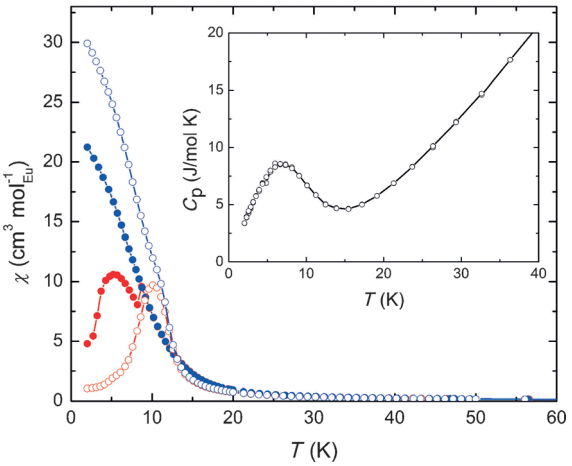

Figure 2. Magnetic susceptibility χ per mol Eu as a function of temperature for $H = 10$ Oe (open circles) and $H = 1000$ Oe (filled circles). Zero-field-cooled (ZFC) and field-cooled (FC) curves are in red and blue, respectively. The inset shows the specific heat capacity as a function of temperature.

two atoms very different in size demonstrates the flexibility of the $Sr_{6.3}Mg_{16.7}Si_{13}$-type structure.

Figure 2 shows the specific heat capacity and the magnetic susceptibility as a function of temperature at magnetic fields of 10 and 1000 Oe. The deviation between the field-cooled (FC) and zero-field-cooled (ZFC) susceptibility loops indicates a frustrated magnetic system. This has been often observed for RE–AE tetralides (AR = alkaline earth) which exhibit metallic behavior and trigonal coordination of the Zintl anions by cations.[9,11] The magnetic susceptibility can be modeled by a Curie–Weiss and a Pauli function (CWP) $\chi = [C/(T-\Theta)] + \chi_0$. The parameter χ_0, a temperature-independent value, represents a combination of the Pauli paramagnetism of the conduction electrons and the diamagnetic contribution of paired electrons. The experimental magnetic moment of 7.98(1) μ_B per Eu^{2+} cation is very close to the theoretical value of 7.94 μ_B. The curvature of the susceptibility exhibits a transition from paramagnetism to a frustrated magnetic system at 11 K. This temperature corresponds exactly to the value of Θ, which is a linear combination of all coupling terms. This phase transition is also visible by the kink in the specific heat curve (Figure 2, inset).

Investigations of the band structure by means of density functional calculations carried out on the theoretical model $Eu_8Mg_{15}Si_{13}$ reveal, consistent with the band structure of the isostructural $Ba_5Mg_{18}Si_{13}$,[7] a density of states (DOS) at the Fermi level (Figure 3). This arises mainly from the p states of the $[Si_4]$ unit. The resulting metallic behavior is a typical property of Zintl phases with ecliptically stacked planar anions.[9] It is therefore most likely that the magnetic coupling between the local moments of the europium cations is determined by the exchange interaction through the conduction electrons according to Rudermann, Kittel, Kasuya, and Yosida (RKKY).[12]

The Fermi surface in Figure 3 indicates anisotropy in the electrical conductivity. Consequently, anisotropic magnetoresistivity can be assumed for the $Eu_{5+x}Mg_{18-x}Si_{13}$ ($x = 2.2$).

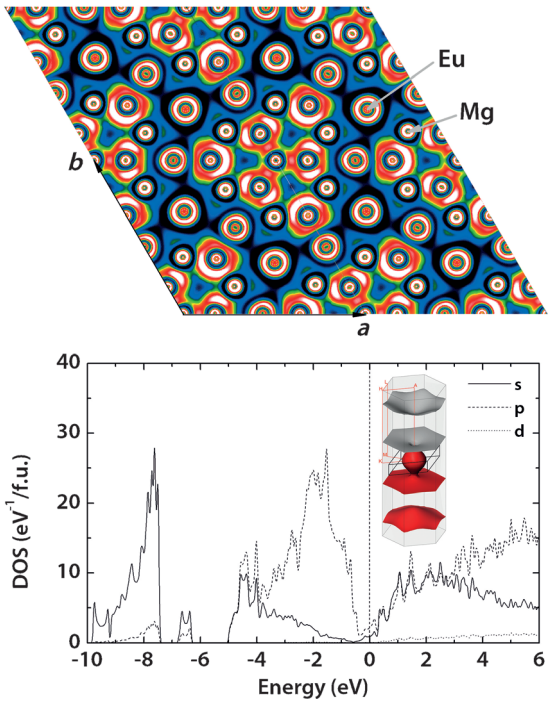

Figure 3. Electron localization function ELF (top; the color coding follows the usual scheme; light colors indicate areas of high localization), density of states, and Fermi surface (bottom) of $Eu_8Mg_{15}Si_{13}$ assuming a full occupancy of the 3f site. Europium atoms were replaced by strontium atoms in the calculations.[11] f.u. = formula unit.

For clarity, the electron localization function (ELF) is illustrated in Figure 3. The Si–Si bonds between the central and terminal atoms are clearly visible.

The electrical resistivity as a function of temperature at different fields is depicted in Figure 4. At higher temperatures and without external field, $Eu_{5+x}Mg_{18-x}Si_{13}$ ($x = 2.2$) displays metallic behavior similar to that of the isostructural phase $Sr_{5+x}Mg_{18-x}Si_{13}$. However, the curve shows a deviation from linearity in the low-temperature regime leading to a resistivity

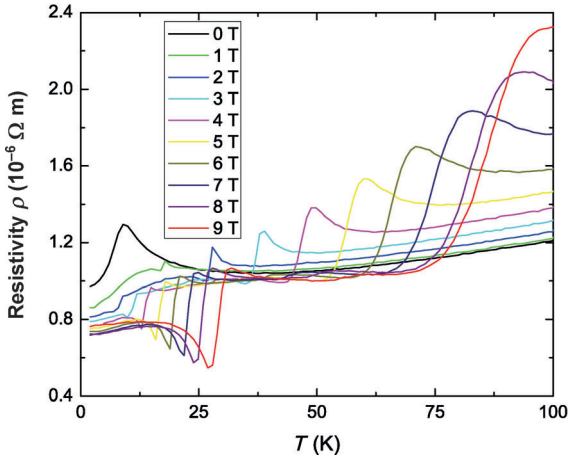

Figure 4. Electrical resistivity of $Eu_{5+x}Mg_{18-x}Si_{13}$ ($x = 2.2$) as a function of temperature from 0 to 100 K and different magnetic fields from 0 to 9 T.

maximum at 9 K. The rise in resistivity is consistent with the phase transition at 11 K (Figure 2). When an external magnetic field is applied, the resistivity maximum decreases, just as it does for normal MR materials, and the MR value reaches −40% at 9 T and 9 K. In contrast to commonly known CMR materials, the resistivity values of $Eu_{5+x}Mg_{18-x}Si_{13}$ ($x = 2.2$) do not converge under applied and zero-field. After the MR value has reached a new maximum of −48% at 27 K and 9 T, an inversion of the sign appears at 31 K and 9 T. The MR increases subsequently and reaches a value of 92%. at 100 K and 9 T.

Suzuki et al.[13] also observed a field-dependent inversion of the magnetoresistivity in their studies of the anisotropic resistivity of single crystals of Ca_2RuO_4 which were, however, conducted under high pressure (1.9 GPa). They suggested that the origin of this behavior is the tunnel magnetoresistance through the metallic domains.

A possible explanation for the MR behavior of $Eu_{5+x}Mg_{18-x}Si_{13}$ ($x = 2.2$) can be found in the physical investigation on the binary Zintl phase EuB_6 described by Ott et al.[14]. The compound is a highly-doped n-type semiconductor with B_6 und Eu vacancies as the corresponding donors and acceptors. The defects are the source of the charge carriers in the conduction band whose Fermi energy depends on the temperature and the applied magnetic field. This may also be the case for the title compound, because the lability of the $[E_4]^{10-}$ anion (E = Si, Ge) can lead to metallic or semiconducting behavior.[7,9]

We have synthesized the new compound $Eu_{5+x}Mg_{18-x}Si_{13}$ ($x = 2.2$) and observed an unusual magnetoresistive behavior. Contrary to already known MR materials, the magnetoresistivity exhibits a maximum at low temperatures. The MR value shows temperature- and field-dependency which also affects its sign. One can speak in this case of an inversion of the magnetoresistive effect. The influence of the europium concentration on the magnetoresistivity will be a topic of future investigations.

Experimental Section

$Eu_{5+x}Mg_{18-x}Si_{13}$ ($x = 2.2$) was synthesized from pure elements (magnesium 99.9 wt% Aldrich; europium 99.9 wt% Smart Elements; silicon lumps 99.9999 wt% Aldrich) in niobium crucibles under inert atmosphere. Prior to the reaction, magnesium and europium were redistilled twice under high-vacuum conditions. The starting materials were mixed in the stoichiometric ratio and prereacted in a high-frequency furnace at 1020 °C for 5 min. In order to achieve better homogeneity, the sample was subsequently ground, pressed into a pellet, and further annealed at 800 K for 5 days. The product is silver-metallic and decomposes upon contact with water. Powder X-ray diffraction experiments showed that the product is stable on air for several months. High-quality single crystals were selected under the optical microscope and sealed in double-walled capillaries for single-crystal X-ray diffraction experiments.

Magnetic measurements were performed on 30 mg of the sample by means of a superconducting quantum interference device (SQUID) by Quantum Design. Each temperature point of a scan was measured ten times and the magnetic moment was averaged for three scans.

Specific heat measurements under zero-field were conducted on a pressed pellet of the sample with the aid of a Physical Properties Measurement System QD-PPMS 9 by Quantum Design. The standard configuration of this system has a resolution of 10 nJ K^{-1} at 2 K and can be operated within the temperature range of 1.9–400 K.

Electrical resistivity measurements were also conducted on a pressed pellet. That pellet was additionally annealed at 923 K for 5 days under inert conditions in order to prevent an overestimation of grain–boundary effects. The measurements were recorded every 0.5 K with the standard four-point-van-der-Pauw method within the temperature range of 2–300 K for magnetic fields from 0 to 9 T.

The chemical analysis for possible niobium impurities by means of LA-ICP-MS showed concentrations below 0.005%.[18]

Received: November 12, 2012
Published online: January 10, 2013

Keywords: europium · magnetism · magnetoresistance · spintronics · zintl phases

[1] a) N. Baibich, J. M. Broto, A. Fert, F. N. Van Dau, F. Petroff, P. Etienne, G. Creuzet, A. Friederich, J. Chazelas, *Phys. Rev. Lett.* **1988**, *61*, 2472–2475; b) G. Binasch, P. Grünberg, F. Saurenbach, W. Zinn, *Phys. Rev. B* **1989**, *39*, 4828–4830.

[2] R. E. Camley, J. Barnaś, *Phys. Rev. Lett.* **1989**, *63*, 664–667.

[3] a) A. P. Ramirez, R. J. Cava, J. Krajewski, *Nature* **1997**, *386*, 156–159; b) M. A. Subramanian, B. H. Toby, A. P. Ramirez, W. J. Marshall, A. W. Sleight, G. H. Kwei, *Science* **1996**, *273*, 81–84; c) R. von Helmolt, J. Wecker, B. Holzapfel, L. Schultz, K. Samwer, *Phys. Rev. Lett.* **1993**, *71*, 2331–2333.

[4] a) E. Zintl, A. Harder, *Z. Phys. Chem. Abt. A* **1931**, *154*, 47; b) E. Zintl, W. Dullenkopf, *Z. Phys. Chem. Abt. B* **1932**, *16*, 195; c) E. Zintl, *Angew. Chem.* **1939**, *52*, 1–6; d) W. Klemm, *Festkörperprobleme*, Vieweg, Braunschweig, **1963**; e) R. Nesper, *Prog. Solid State Chem.* **1990**, *20*, 1–45; f) T. F. Faessler, *Zintl Phases*, Springer, Berlin, **2011**.

[5] a) J. Y. Chan, S. M. Kauzlarich, P. Klavins, R. N. Shelton, D. J. Webb, *Chem. Mater.* **1997**, *9*, 3132–3135; b) J. Y. Chan, S. M. Kauzlarich, P. Klavins, R. N. Shelton, D. J. Webb, *Phys. Rev. B* **1998**, *57*, R8103–R8106; c) A. C. Payne, M. M. Olmstead, S. M. Kauzlarich, D. J. Webb, *Chem. Mater.* **2001**, *13*, 1398–1406; d) N. Tsujii, C. A. Uvarov, P. Klavins, T. Yi, S. M. Kauzlarich, *Inorg. Chem.* **2012**, *51*, 2860–2866; e) H. Hartmann, K. Berggold, S. Jodlauk, I. Klassen, K. Kordonis, T. Fickenscher, R. Poettgen, A. Freimuth, T. Lorenz, *J. Phys. Condens. Matter* **2005**, *17*, 7731–7741.

[6] Crystal structure data for $Eu_{5+x}Mg_{18-x}Si_{13}$ ($x = 2.2$) at $T = 293$ K: hexagonal $P\bar{6}2m$ (no. 189), $a = 14.6356(14)$ Å, $c = 4.4111(6)$ Å, $V = 818.3(2)$ Å^3, $\rho = 3.73$ g cm^{-3}, $Z = 1$, $\theta_{max} = 25.25°$, 45 parameters refined, 7323 measured reflections, 606 unique reflections, $R1 = 0.0088$, $wR2 = 0.0221$, max./min. residual electron density: $+0.318/-0.369$ e Å^{-3}. Diffractometer: Bruker SMART Platform (MoK_α radiation, Graphite monochromator). The data were integrated with the SAINT program[16] and corrected for Lorentz factor, polarization, air absorption, and absorption due to the path length through the detector face plate. The structure was solved with the Patterson method.[17] Further details on the crystal structure investigations may be obtained from the Fachinformationszentrum Karlsruhe, 76344 Eggenstein-Leopoldshafen, Germany (fax: (+49) 7247-808-666; e-mail: crysdata@fiz-karlsruhe.de), on quoting the depository number CSD-425218.

[7] R. Nesper, S. Wengert, F. Zürcher, A. Currao, *Chem. Eur. J.* **1999**, *5*, 3382–3389.

[8] H. G. von Schnering, R. Nesper, J. Curda, K.-F. Tebbe, *Angew. Chem.* **1980**, *92*, 1070–1070; *Angew. Chem. Int. Ed. Engl.* **1980**, *19*, 1033–1034.

[9] A. Slabon, E. Cuervo-Reyes, C. Kubata, C. Mensing, R. Nesper, *Z. Anorg. Allg. Chem.* **2012**, *638*, 2020 – 2028.
[10] a) F. Weitzer, Y. Prots, W. Schnelle, K. Hiebl, Y. Grin, *J. Solid State Chem.* **2004**, *177*, 2115 – 2121; b) A. Slabon, E. Cuervo-Reyes, C. Kubata, M. Wörle, C. Mensing, R. Nesper, *Z. Anorg. Allg. Chem.* **2012**, *638*, 1417 – 1423.
[11] E. Cuervo-Reyes, A. Slabon-Turski, C. Mensing, R. Nesper, *J. Phys. Chem. C* **2012**, *116*, 1158 – 1164.
[12] C. Kittel, *Solid State Phys.* **1969**, *22*, 1.
[13] F. Nakamura, R. Nakai, T. Takemoto, M. Sakaki, T. Suzuki, P. L. Alireza, S. Nakatsuji, Y. Maeno, *Phys. Rev. B* **2009**, *80*, 193103.
[14] G. A. Wigger, R. Monnier, H. R. Ott, D. P. Young, Z. Fisk, *Phys. Rev. B* **2004**, *69*, 125118.
[15] M. McElfresh, *Fundamentals of Magnetism and Magnetic Measurements, Featuring Quantum Design's Magnetic Property Measurement System*, Quantum Design, New York, **1994**.
[16] SAINT Version 4.05. Siemens Analtyical X-Ray Instruments, Madison, WI, **1996**.
[17] G. M. Sheldrick, *Acta Crystallogr. Sect. A* **2008**, *64*, 112 – 122.
[18] D. Günther, S. E. Jackson, H. P. Longerich, *Spectrochim. Acta Part B* **1999**, *54*, 381.

